SU(3) Topology of Magnon-Phonon Hybridization in 2D Antiferromagnets

Shu Zhang,[1,2,*] Gyungchoon Go,[3] Kyung-Jin Lee,[3,4] and Se Kwon Kim[5,†]
[1]Department of Physics and Astronomy, Johns Hopkins University, Baltimore, Maryland 21218, USA
[2]Department of Physics and Astronomy, University of California, Los Angeles, California 90095, USA
[3]Department of Materials Science and Engineering, Korea University, Seoul 02841, Korea
[4]KU-KIST Graduate School of Converging Science and Technology, Korea University, Seoul 02841, Korea
[5]Department of Physics and Astronomy, University of Missouri, Columbia, Missouri 65211, USA

(Received 1 October 2019; accepted 27 March 2020; published 9 April 2020)

Magnon-phonon hybrid excitations are studied theoretically in a two-dimensional antiferromagnet with an easy axis normal to the plane. We show that two magnon bands and one phonon band are intertwined by the magnetoelastic coupling through a nontrivial SU(3) topology, which can be intuitively perceived by identifying a skyrmion structure in the momentum space. Our results are insensitive to lattice details and generally applicable to two-dimensional antiferromagnets. We show this by developing a continuum theory as the long-wavelength approximation to the tight-binding model. The theoretical results can be probed by measuring the thermal Hall conductance as a function of the temperature and the magnetic field. We envision that the magnetoelastic coupling in antiferromagnets can be a promising venue in search of various topological excitations, which cannot be found in magnetic or elastic models alone.

DOI: 10.1103/PhysRevLett.124.147204

Antiferromagnets have recently emerged as promising material platforms in spintronics [1–3]. Due to the absence of the stray field and the intrinsic timescale at THz, antiferromagnet-based devices can be packed denser and operate at higher speeds than conventional ferromagnet-based GHz devices, which interact with each other via a stray field. In particular, antiferromagnets are expected to provide efficient spin-transport channels between spintronics devices, as observed in the antiferromagnetic insulator chromia [4] and haematite [5].

Parallel to the emergence of antiferromagnetic spintronics, there has been significant effort in identifying novel topological excitations in magnets, driven by both fundamental interest and their practical use as robust transport channels. Topological magnons have been identified in several types of magnets, see Refs. [6–17] for examples. Going beyond previous work on topological magnons, hybrid excitations of magnons and phonons are also shown to be topological in certain magnets, in presence of the Dzyaloshinskii-Moriya interaction (DMI) [18], the dipolar coupling [19], or the exchange magnetorestriction [20]. Some of us have recently shown [21] that a topologically nontrivial magnon-phonon hybridization can be induced in a square-lattice ferromagnet—even in the absence of inversion-symmetry-breaking DMI or long-range dipolar coupling—by a magnetoelastic coupling, which is expected to generally exist in magnets with crystalline anisotropy [22].

In this Letter, we address the topological effect of the magnetoelastic coupling [23] in a square-lattice *antiferromagnet*, where a minimal model to describe magnon-phonon hybrid excitations requires three quasiparticles. Different from the SU(2) topology of the ferromagnetic case with two bands [21], they possess an enriched topological structure of the SU(3) algebra. Aside from directly calculating Chern numbers of excitations bands using the SU(3) formalism, we show that, an intuitive understanding of the band topology can be obtained by identifying a skyrmion structure, where skyrmion numbers are defined through the more familiar SU(2) formalism [24]. The nontrivial topology gives rise to the thermal Hall effect, where the direction of the transverse heat flow can be controlled, as the thermal Hall conductance changes sign upon reversal of the out-of-plane magnetic field, see Fig. 1(a). There has been growing interest in a family of two-dimensional antiferromagnets MPS_3 (M = Mn, Fe, Ni) [25,26], where we propose the thermal Hall effect to be

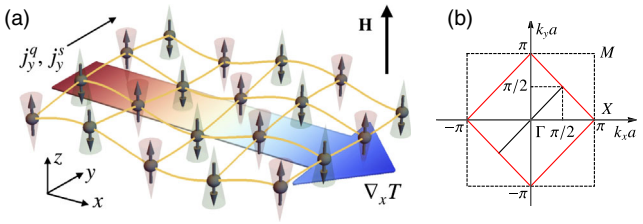

FIG. 1. (a) Magnon-phonon hybrid excitations in a square-lattice antiferromagnet. The system exhibits the thermal Hall effect and the spin Nernst effect, which refer to the generation of a heat current j_y^q (under magnetic field $\mathbf{H}$) and a spin current j_y^s transverse to the applied temperature gradient $\nabla_x T$. (b) The lattice Brillouin zone (dashed black square) and the magnetic Brillouin zone (red square), where a is the lattice constant.

observed due to the magnetoelastic coupling discussed in this work. For experimental comparison, we give a prediction for the dependence of the thermal Hall conductance on the temperature and the magnetic field. Furthermore, by developing a continuum field theory for the magnetic and elastic degrees of freedom, we show that our results are generally applicable to two-dimensional antiferromagnets. We envision antiferromagnets serving as versatile platforms to realize various multiband topological insulators, where magnon-phonon excitations can be used for robust information transport in spintronics. The broader implications of our work are discussed at the end of the Letter.

Model.—We study harmonic excitations of the Hamiltonian

$$H = H_m + H_e + H_{me} \tag{1}$$

on a square lattice, which describes two subsystems—magnetic and elastic—and the interaction between them.

The magnetic interactions include the nearest-neighbor antiferromagnetic Heisenberg exchange, the easy-axis anisotropy, and the Zeeman coupling to an external magnetic field $\mathbf{H} = H\hat{\mathbf{z}}$:

$$H_m = J\sum_{\langle \ell\ell'\rangle} \mathbf{S}_\ell \cdot \mathbf{S}_{\ell'} - \frac{K}{2}\sum_\ell S_\ell^{z2} - h\sum_\ell S_\ell^z, \tag{2}$$

where $\langle \ell\ell'\rangle$ runs over all pairs of nearest neighbors, $J, K > 0$ are respectively the exchange constant and the anisotropy coefficient, and the Zeeman coupling is $h = \mu_B g H$ with the Bohr magneton μ_B and the Landé g factor, g. One of the two time-reversal-related Néel ground states has the spin configuration $\mathbf{S}_{i\in A} = S\hat{\mathbf{z}}$ and $\mathbf{S}_{j\in B} = -S\hat{\mathbf{z}}$, as shown in Fig. 1(a). We study magnon excitations by the Holstein-Primakoff approach [27],

$$H_m = \sum_{\mathbf{k}} (\epsilon_{\mathbf{k}}^{m+}\alpha_{\mathbf{k}}^\dagger\alpha_{\mathbf{k}} + \epsilon_{\mathbf{k}}^{m-}\beta_{\mathbf{k}}^\dagger\beta_{\mathbf{k}}) + \text{const.}, \tag{3}$$

where the wave vector $\mathbf{k}$ is summed over the first magnetic Brillouin zone shown in Fig. 1(b). There are two magnon bands with dispersion relations $\epsilon_{\mathbf{k}}^{m\pm} = S\sqrt{(zJ+K)^2 - (J\gamma_{\mathbf{k}})^2} \pm h$, where $z = 4$ is the coordinate number and $\gamma_{\mathbf{k}} = 2[\cos(k_x a) + \cos(k_y a)]$. The bosonic operator $\alpha_{\mathbf{k}}^\dagger$ ($\beta_{\mathbf{k}}^\dagger$) creates a magnon with $S^z = -1$ ($+1$), which is a good quantum number because of the rotational symmetry of the Hamiltonian (2). We assume $h \lesssim S\sqrt{8JK}$ so that magnons have finite gaps.

For the Hamiltonian describing the lattice dynamics, we consider the out-of-plane component u_ℓ^z of the displacement vector $\mathbf{u}_\ell$, which is the only component that later enters the magnon-phonon coupling:

$$H_e = \frac{1}{2M}\sum_\ell (p_\ell^z)^2 + \frac{\lambda}{2}\sum_{\langle \ell\ell'\rangle} (u_\ell^z - u_{\ell'}^z)^2, \tag{4}$$

where M is the atom mass, $p_\ell^z = M\dot{u}_\ell^z$ is the conjugate momentum, and λ is the spring constant between nearest neighbors. The quantization of phonon excitations yields

$$H_e = \sum_{\mathbf{k}} (\epsilon_{\mathbf{k}}^{p-}\eta_{\mathbf{k}}^\dagger\eta_{\mathbf{k}} + \epsilon_{\mathbf{k}}^{p+}\zeta_{\mathbf{k}}^\dagger\zeta_{\mathbf{k}}) + \text{const.}, \tag{5}$$

where phonon dispersion relations are $\epsilon_{\mathbf{k}}^{p\pm} = \hbar\omega_0\sqrt{z \pm \gamma_{\mathbf{k}}}$ with characteristic frequency $\omega_0 = \sqrt{\lambda/M}$. In the reduced (magnetic) Brillouin zone, we obtain two phonon modes, the acoustic branch $\eta_{\mathbf{k}}$ and the optical branch $\zeta_{\mathbf{k}}$.

Our study focuses on the interaction between the spin and the elastic strain, which will be shown later to induce nontrivial topology to the excitation bands. As was pointed out by Kittel [23],

$$H_{me} = \kappa \sum_{\ell\in A,B}\sum_\delta S_\ell^z (\mathbf{S}_\ell \cdot \hat{\mathbf{e}}_\delta)(u_\ell^z - u_{\ell+\delta}^z), \tag{6}$$

where κ is the magnetoelastic coupling constant and $\hat{\mathbf{e}}_\delta$ is a unit vector pointing along the bond connecting nearest neighbors. For our magnetic ground state, this term (6) is the leading order approximation to the magnetoelastic energy.

When $\kappa = 0$, the acoustic phonon intersects magnon bands at rings of wave vectors as shown in Figs. 2(a)–2(c). We treat the magnetoelastic coupling as a perturbation, the most prominent effect of which is to lift the degeneracy at band crossings. Therefore, the magnetoelastic Hamiltonian (6) expressed in magnon and phonon operators is dominated by terms conserving the total number of quasiparticles,

$$\begin{aligned} H_{me} \approx \kappa \sum_{\mathbf{k}} \sum_{b=+,-} \{ & v_{\mathbf{k}}^b \chi_{\mathbf{k}}^b [i\sin(k_x a)(\alpha_{\mathbf{k}}^\dagger + b\beta_{\mathbf{k}}^\dagger) \\ & - \sin(k_y a)(\alpha_{\mathbf{k}}^\dagger - b\beta_{\mathbf{k}}^\dagger)] + \text{H.c.}\}, \end{aligned} \tag{7}$$

where $\chi_{\mathbf{k}}^+ = \zeta_{\mathbf{k}}$, $\chi_{\mathbf{k}}^- = \eta_{\mathbf{k}}$, $v_{\mathbf{k}}^\pm = \hbar S^{3/2}\sqrt{1/2M\epsilon_{\mathbf{k}}^{p\pm}} \times (\sinh\vartheta_{\mathbf{k}} \pm \cosh\vartheta_{\mathbf{k}})$ with $\tanh 2\vartheta_{\mathbf{k}} = -J\gamma_{\mathbf{k}}/(zJ+K)$.

The full Hamiltonian (1) thus becomes a tight-binding model for magnon-phonon hybrid excitations. By exact diagonalization, we find that the magnetoelastic coupling gives rise to the so-called avoided crossing features in excitation bands, as shown in Figs. 2(d)–2(f). The degree of hybridization is reflected by the spin number $S_n^z(\mathbf{k}) = \langle\phi_n(\mathbf{k})|(\beta_{\mathbf{k}}^\dagger\beta_{\mathbf{k}} - \alpha_{\mathbf{k}}^\dagger\alpha_{\mathbf{k}})|\phi_n(\mathbf{k})\rangle$, where $\phi_n(\mathbf{k})$ is the wave function of the band with the eigenenergy $E_n(\mathbf{k})$.

SU(3) topology.—To study the band topology, it is adequate to consider the three-band Hamiltonian [28]

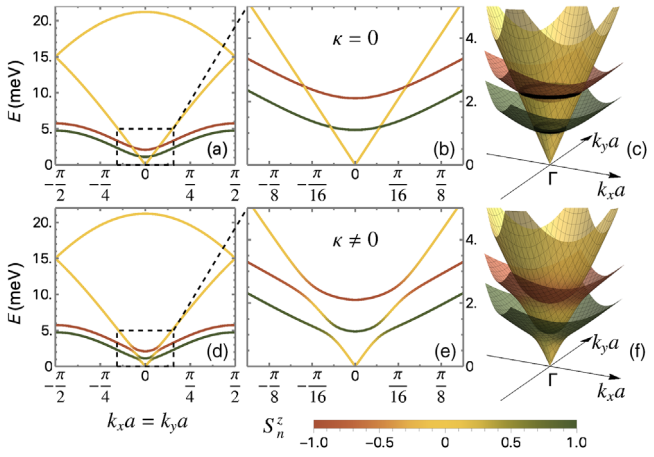

FIG. 2. Dispersion relations of excitation bands. (a)–(c) In the absence of the magnetoelastic coupling. The green and the red lines depict the $S^z = 1$ magnons and the $S^z = -1$ magnons, respectively. The yellow lines depict phonons. (d)–(f) Hybridization of magnons and the acoustic phonon in the presence of the magnetoelastic coupling $\kappa = 0.8$ meV/Å. The color represents the value of S_n^z of the nth band at each momentum. Parameters used are these: $S = 5/2$, $J = h = 0.5$ meV, $K = 0.1$ meV, and $\hbar\omega_0 = 7.5$ meV.

$H_3 = \sum_{\mathbf{k}} \psi_{\mathbf{k}}^\dagger \mathcal{H}_{\mathbf{k}} \psi_{\mathbf{k}}$, with the operator $\psi_{\mathbf{k}} = (\alpha_{\mathbf{k}}, \beta_{\mathbf{k}}, \eta_{\mathbf{k}})^T$ and the hopping matrix

$$\mathcal{H}_{\mathbf{k}} = \begin{pmatrix} \epsilon_{\mathbf{k}}^{m+} & 0 & C_{\mathbf{k}} \\ 0 & \epsilon_{\mathbf{k}}^{m-} & C_{\mathbf{k}}^* \\ C_{\mathbf{k}}^* & C_{\mathbf{k}} & \epsilon_{\mathbf{k}}^{p-} \end{pmatrix}, \tag{8}$$

with the magnon-phonon coupling $C_{\mathbf{k}} = \kappa v_{\mathbf{k}}^-[i\sin(k_x a) - \sin(k_y a)]$. The three-band tight-binding model is naturally described by the algebra of the SU(3) group. By making a similarity transformation and eliminating the trace, the Bloch Hamiltonian (8) becomes

$$\tilde{\mathcal{H}}_{\mathbf{k}} = h\lambda_2 + \sqrt{2}\kappa v_{\mathbf{k}}^-[\sin(k_x a)\lambda_5 - \sin(k_y a)\lambda_7] + \frac{1}{2\sqrt{3}}(\epsilon_{\mathbf{k}}^{m+} + \epsilon_{\mathbf{k}}^{m-} - 2\epsilon_{\mathbf{k}}^{p-})\lambda_8, \tag{9}$$

where λs are Gell-Mann matrices [29] for SU(3) group akin to Pauli matrices for SU(2) group.

Following the method developed by Barnett *et al.* [30], we compute the Berry curvature $\Omega_n^z(\mathbf{k})$ and the Chern number C_n associated with each band directly from the Bloch Hamiltonian (9). For $h > 0$, we find the Chern numbers to be $(+1, -2, +1)$, see Figs. 3(a)–3(c). All Chern numbers flip their signs when the magnetic field is in the opposite direction, see Figs. 3(h)–3(j) for $h < 0$. As shown in Figs. 3(k)–3(m), a topological phase transition happens at $h = 0$, when the band gaps close at both Γ point and the boundary of the Brillouin zone.

We notice that $(\lambda_2, \lambda_5, \lambda_7)$ forms the spin-1 representation of angular momentum operators. Three-band hopping models enjoying such a SU(2) subalgebra have been well understood [31–33], where Chern numbers are $(-c, 0, c)$ with $c \in \mathbb{Z}$. The presence of λ_8 enriches the band topology of our model. Similar cases have been previously studies in cold atom systems [30,34], where formalism with more mathematical rigor is discussed.

Here, we achieve an understanding of the band topology more intuitively, with the help of the skyrmion structure in the familiar two-band theories. For $\kappa a \ll h$, nonzero Berry curvatures concentrate in the vicinity of avoided crossings, while the two rings of momenta satisfying $\epsilon_{\mathbf{k}}^{m\pm} = \epsilon_{\mathbf{k}}^{p-}$ are relatively separated from each other.

Let us take the example of $h > 0$. For wave vectors near the band crossing $\epsilon_{\mathbf{k}}^{m-} = \epsilon_{\mathbf{k}}^{p-}$, the prominent topological effect should occur between the two crossing bands, which motivates us to write the Bloch Hamiltonian (8) in the following form:

$$\mathcal{H}_{\mathbf{k}} = \begin{pmatrix} \epsilon_{\mathbf{k}}^{m+} & 0 \\ 0 & \frac{1}{2}(\epsilon_{\mathbf{k}}^{m-} + \epsilon_{\mathbf{k}}^{p-})I_2 + \mathbf{d}(\mathbf{k})\cdot\boldsymbol{\sigma} \end{pmatrix} + \mathcal{V}_{\mathbf{k}}, \tag{10}$$

where $\boldsymbol{\sigma} = (\sigma^x, \sigma^y, \sigma^z)$ are Pauli matrices, $\mathbf{d}(\mathbf{k}) = [-\kappa v_{\mathbf{k}}^- \sin(k_y a), \kappa v_{\mathbf{k}}^- \sin(k_x a), (\epsilon_{\mathbf{k}}^{m-} - \epsilon_{\mathbf{k}}^{p-})/2]$. Here, $\mathcal{V}_{\mathbf{k}}$ is a perturbation term that does not participate in opening the gap between the two bands ($\epsilon_{\mathbf{k}}^{m-}$ and $\epsilon_{\mathbf{k}}^{p-}$) and thus can be neglected for now. A skyrmion with topological charge $Q = +1$ [see Fig. 3(e)] emerges in the unit vector field $\hat{\mathbf{d}}(\mathbf{k}) = \mathbf{d}(\mathbf{k})/|\mathbf{d}(\mathbf{k})|$, where

$$Q = \frac{1}{4\pi}\int dk_x \int dk_y \hat{\mathbf{d}}(\mathbf{k})\cdot\left(\frac{\partial\hat{\mathbf{d}}(\mathbf{k})}{\partial k_x}\times\frac{\partial\hat{\mathbf{d}}(\mathbf{k})}{\partial k_y}\right). \tag{11}$$

According to the SU(2) model for two bands gapped by $\mathbf{d}(\mathbf{k})$, the lower (upper) band has Chern number $+Q$ $(-Q)$. Similarly, around $\epsilon_{\mathbf{k}}^{m+} = \epsilon_{\mathbf{k}}^{p-}$, the Berry curvature is determined by an anti-skyrmion with $Q = -1$ [see Fig. 3(d)]. Together, the skyrmion and antiskyrmion structure gives a Chern number distribution $(+1, -2, +1)$. For $h < 0$, the only difference lies at $\epsilon_{\mathbf{k}}^{m-} > \epsilon_{\mathbf{k}}^{m+}$. The Chern numbers are thus reversed, with the skyrmion structure shown in Figs. 3(f), 3(g). The consideration of the skyrmion structure is consistent with the homotopy theory for an SU(3) matrix with a fixed set of eigenvalues [35,36]: $\pi_2\{\mathrm{SU}(3)/[\mathrm{U}(1)\times\mathrm{U}(1)]\} \simeq \pi_1[\mathrm{U}(1)] \times \pi_1[\mathrm{U}(1)] = \mathbb{Z}\times\mathbb{Z}$.

Experimental applications.—The nontrivial band topology gives rise to thermal Hall effect, which can be observed in experiments. A current of magnon-phonon excitations drifting under a temperature gradient acquires a transverse component in presence of the fictitious magnetic field $\Omega_n^z(\mathbf{k})$. The thermal Hall conductance is given by [37,38] $\kappa_T = -(k_B^2 T/\hbar)\sum_n \int d^2\mathbf{k}\Omega_n^z(\mathbf{k})c_2[\rho_n(\mathbf{k})]$, where

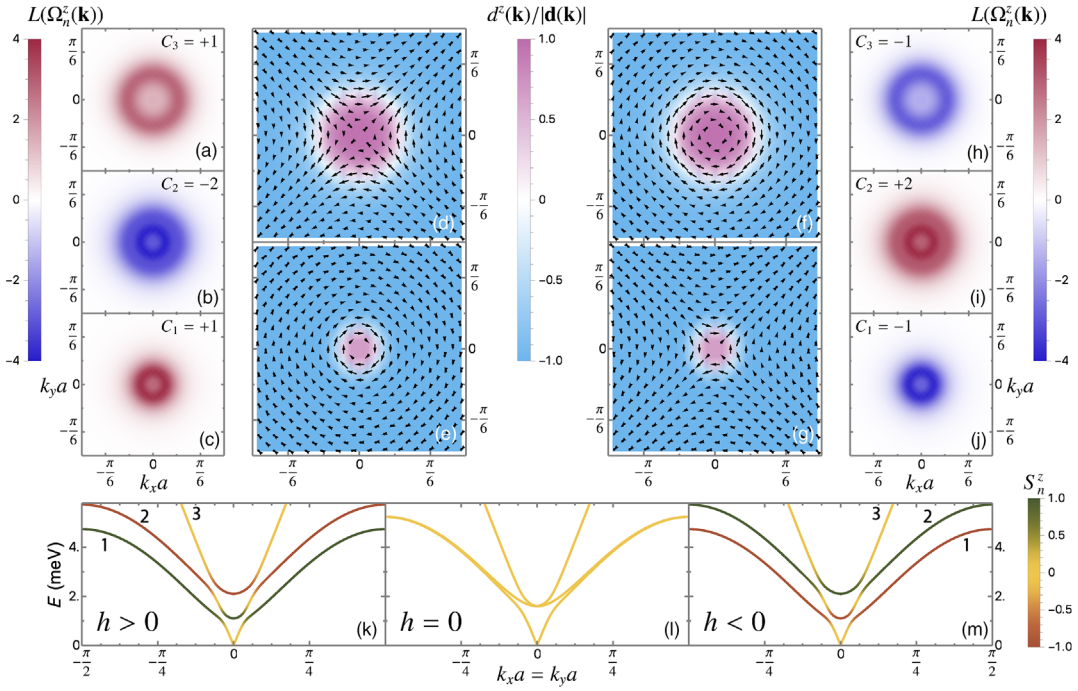

FIG. 3. Topological properties of magnon-phonon hybrid excitations. Berry curvatures Ω_n^z of excitation bands for $h > 0$ (a)–(c) and $h < 0$ (h)–(j) are plotted in log scale [21] $L(\Omega_n^z) = \mathrm{sign}(\Omega_n^z)\log(1 + |\Omega_n^z|)$. The corresponding skyrmion structures are shown for $h > 0$ (d), (e) and $h < 0$ (f), (g), where black arrows are in-plane components of $\mathbf{d}(\mathbf{k})$. Same parameters are used as in Fig. 2. A topological phase transition (k)–(m) occurs at $h = 0$ when band gaps close. See the main text for detailed discussions.

$c_2(\rho) = (1+\rho)\ln^2[(1+\rho)/\rho] - \ln^2\rho - 2\mathrm{Li}_2(-\rho)$, $\rho_n(\mathbf{k}) = 1/[\exp(E_n(\mathbf{k})/k_BT) - 1]$ is the Bose-Einstein distribution function, and $\mathrm{Li}_2(z)$ is the polylogarithm function.

We estimated a set of parameters for $MnPS_3$ to plot the temperature T and magnetic field H dependence of the thermal Hall conductance in Fig. 4. A Mn ion has mass $M = 55$ u and spin $S = 5/2$. The lattice constant is $a = 6.1$ Å. We set $\hbar\omega_0 = 7.5$ meV, resulting in a phonon velocity $\sim$5 km/s; magnetic parameters [39,40] $zJ = 4$ meV and $K = 0.01$ meV, yielding a small magnon gap $\sim$0.7 meV; the Landé g factor $g = -2.0$; and the magnetoelastic coupling $\kappa = 0.2$ meV/Å, giving $2\kappa S^2/a^2 \sim 11$ J/cm^3, in the same order of magnitude with Kittel's

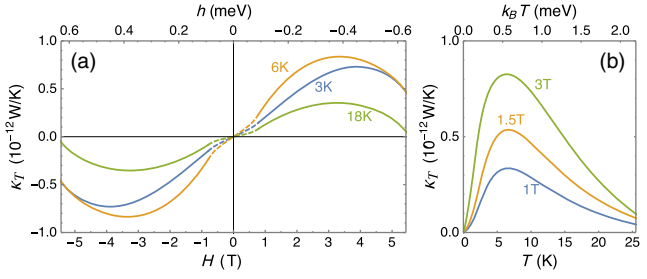

FIG. 4. The magnetic field dependence (a) and temperature dependence (b) of the thermal Hall conductance κ_T. The dashed lines are extrapolations from calculation. Parameters and estimated for $MnPS_3$, see main text.

estimation [22]. The resulting thermal Hall conductance has a magnitude comparable to the observed values in Ref. [41], thus is within the current experiment reach.

The antisymmetric feature of κ_T under the magnetic field can be of practical interest in designing spincaloritronic devices with reversal thermal current. Since the magnetoelastic coupling explicitly couples the spin orientation and the lattice wave vector [see Eq. (12) in the continuum theory], the spin Nernst effect [42,43] is also expected to be observable. According to the bulk-edge correspondence [44,45], there are two edge modes carrying a net spin current.

Applicability to general 2D antiferromagnets.—The nontrivial SU(3) band topology in magnon-phonon hybrid excitations is not limited to a square-lattice system. We expect it to be a rather general phenomenon in two-dimensional antiferromagnets. This is demonstrated by developing a continuum theory, which is equivalent to the tight-binding model in the low-energy and long-wavelength limit (with $\kappa a \ll S\sqrt{2J^3/K} \ll \hbar\omega_0$).

We study the dynamics of two slowly varying fields—the unit-vector staggered spin $\mathbf{n}(\mathbf{r}, t) = (\mathbf{S}_A - \mathbf{S}_B)/2S = \hat{\mathbf{z}} + \delta\mathbf{n}(\mathbf{r}, t)$ [46], and the lattice displacement $u^z(\mathbf{r}, t)$. They are coupled through the energy density

$$\mathcal{H}_{me} = -\frac{2\kappa S^2}{a}\mathbf{n}\cdot\nabla u^z. \tag{12}$$

Dispersion relations of the magnon-phonon hybrid excitations are revealed by their coupled equations of motion, which can be derived from the action

$$\mathcal{S}[\Psi] \approx \frac{1}{2}\int d^2\mathbf{k} \int d\omega \Psi^{\dagger}_{\mathbf{k},\omega}(E - \mathcal{G}_{\mathbf{k},\omega})\Psi_{\mathbf{k},\omega}, \quad (13)$$

where the operator $\Psi_{\mathbf{k},\omega}$ is the Fourier transform of the field operator $[\psi^+(\mathbf{r},t),\psi^-(\mathbf{r},t),u^z(\mathbf{r},t)]^T$ with $\psi^{\pm} = \delta n_x \pm i\delta n_y$; and

$$\mathcal{G}_{\mathbf{k},\omega} = \begin{pmatrix} E_m + h & 0 & \tilde{C}_{\mathbf{k}} \\ 0 & E_m - h & \tilde{C}^*_{\mathbf{k}} \\ \tilde{C}^*_{\mathbf{k}} & \tilde{C}_{\mathbf{k}} & E_p \end{pmatrix} \quad (14)$$

with $E_m = S\sqrt{8JK} + S\sqrt{2J^3/K}a^2(k_x^2 + k_y^2)$, $E_p = \hbar\omega_0 a\sqrt{k_x^2 + k_y^2}$, and $\tilde{C} = -\kappa S^{3/2}(8J/K)^{1/4}\sqrt{a\hbar/2M\omega_0}\times (k_x^2 + k_y^2)^{-1/4}(ik_x - k_y)$. These are exactly the lowest order approximations to elements in the Block Hamiltonian (8), and thus the continuum theory (13) possesses the same band topology with that of square-lattice system: Our results on the nontrivial SU(3) topology of magnon-phonon hybrid excitations and the resultant thermal Hall conductivity are expected to exist generally in two-dimensional antiferromagents regardless of their lattice structures.

Discussion.—We remark on the applicability of our theoretical model more generally. First, we study a classical spin system with an antiferromagnetic order. At a temperature is much lower than the Néel temperature, magnetic excitations are magnons with well-defined dispersions. Second, we have focused on the hybridization between two magnon bands and the acoustic phonon, which is a minimal model for an antiferromagnet. The effect of the magnetoelastic coupling can, of course, be generally considered for more complicated band structures, such as phonons from other displacement components and magnons in noncollinear antiferromagnet. Third, the rotational symmetry around the easy axis is approximate in the low energy limit in a lattice system.

Several features of the magnetoelastic coupling (6) are worth noting in our study. It is linear in magnon operators, as manifested in Eq. (7), thus has a leading order contribution to the excitation spectrum. In the continuum form (12), it has the familiar form of a spin-orbit coupling. Without the requirement of breaking the inversion symmetry, it is expected to exist generally in magnetic systems. In contrast to the widely studied Dzyaloshinskii-Moriya interaction [47,48], the effect of the magnetoelastic coupling (6) is largely unknown. By revealing the nontrivial topology it can induce to magnon-phonon hybrid excitations, we hope to bring more attention to its effects.

The magnetoelastic coupling can serve as a venue in search of various topological excitations, as well as other novel phenomena in the interplay between magnetic and elastic degrees of freedom. For example, nonreciprocal phonons in a magnetic ordered state (as recently observed in Ref. [49]) can be a more generally existing effect [23]; and vice versa, the possibility to use strain to tune magnetic states or mangon properties can be considered [25].

An interesting subject for future study is the effect from the intrinsic quantum mechanical nature of antiferromagnetic magnons, which can be prominent when the spin length is small. Another is the magnon-phonon hybridization engendered by the exchange-type magnetoelastic coupling as in Ref. [20], which could be strong especially in materials exhibit the Jahn-Teller effect [50]. It has been shown that magnon-photon coupling can result similar band repelling effect [51,52]. Our ideology might also be of interest for topological photonics [53] in magnetic systems.

We thank Oleg Tchernyshyov for comments on the manuscript. S. Z. and S. K. K. acknowledge the support by the University of Missouri. S. Z. is also supported by the U.S. DOE Basic Energy Sciences, Materials Sciences and Engineering Award No. DE-SC0019331. S. K. K. is supported by Young Investigator Grant (YIG) from Korean-American Scientists and Engineers Association (KSEA). G. G. is supported by the NRF of Korea (Grant No. NRF–2019R1I1A1A01063594). K.-J. L. acknowledges a support by the National Research Foundation (NRF) of Korea (Grant No. NRF-2017R1A2B2006119).

*suzy@physics.ucla.edu
†kimsek@missouri.edu

[1] T. Jungwirth, X. Marti, P. Wadley, and J. Wunderlich, Nat. Nanotechnol. **11**, 231 (2016).
[2] V. Baltz, A. Manchon, M. Tsoi, T. Moriyama, T. Ono, and Y. Tserkovnyak, Rev. Mod. Phys. **90**, 015005 (2018).
[3] M. B. Jungfleisch, W. Zhang, and A. Hoffmann, Phys. Lett. A **382**, 865 (2018).
[4] W. Yuan, Q. Zhu, T. Su, Y. Yao, W. Xing, Y. Chen, Y. Ma, X. Lin, J. Shi, R. Shindou, X. C. Xie, and W. Han, Sci. Adv. **4**, eaat1098 (2018).
[5] R. Lebrun, A. Ross, S. A. Bender, A. Qaiumzadeh, L. Baldrati, J. Cramer, A. Brataas, R. A. Duine, and M. Kläui, Nature (London) **561**, 222 (2018).
[6] L. Zhang, J. Ren, J.-S. Wang, and B. Li, Phys. Rev. B **87**, 144101 (2013).
[7] R. Shindou, J.-i. Ohe, R. Matsumoto, S. Murakami, and E. Saitoh, Phys. Rev. B **87**, 174402 (2013).
[8] R. Shindou, R. Matsumoto, S. Murakami, and J.-I. Ohe, Phys. Rev. B **87**, 174427 (2013).
[9] A. Mook, J. Henk, and I. Mertig, Phys. Rev. B **90**, 024412 (2014).
[10] S. K. Kim, H. Ochoa, R. Zarzuela, and Y. Tserkovnyak, Phys. Rev. Lett. **117**, 227201 (2016).
[11] S. A. Owerre, J. Phys. Condens. Matter **28**, 386001 (2016).
[12] V. A. Zyuzin and A. A. Kovalev, Phys. Rev. Lett. **117**, 217203 (2016).

[13] K. Nakata, S. K. Kim, J. Klinovaja, and D. Loss, Phys. Rev. B **96**, 224414 (2017).
[14] B. Göbel, A. Mook, J. Henk, and I. Mertig, Phys. Rev. B **95**, 094413 (2017).
[15] S. K. Kim, K. Nakata, D. Loss, and Y. Tserkovnyak, Phys. Rev. Lett. **122**, 057204 (2019).
[16] S. A. Díaz, J. Klinovaja, and D. Loss, Phys. Rev. Lett. **122**, 187203 (2019).
[17] K.-S. Kim, K. H. Lee, S. B. Chung, and J.-G. Park, Phys. Rev. B **100**, 064412 (2019).
[18] X. Zhang, Y. Zhang, S. Okamoto, and D. Xiao, Phys. Rev. Lett. **123**, 167202 (2019).
[19] R. Takahashi and N. Nagaosa, Phys. Rev. Lett. **117**, 217205 (2016).
[20] S. Park and B.-J. Yang, Phys. Rev. B **99**, 174435 (2019).
[21] G. Go, S. K. Kim, and K.-J. Lee, Phys. Rev. Lett. **123**, 237207 (2019).
[22] C. Kittel, Rev. Mod. Phys. **21**, 541 (1949).
[23] C. Kittel, Phys. Rev. **110**, 836 (1958).
[24] X.-L. Qi and S.-C. Zhang, Rev. Mod. Phys. **83**, 1057 (2011).
[25] K. S. Burch, D. Mandrus, and J.-G. Park, Nature (London) **563**, 47 (2018).
[26] M. Gibertini, M. Koperski, A. Morpurgo, and K. Novoselov, Nat. Nanotechnol. **14**, 408 (2019).
[27] T. Holstein and H. Primakoff, Phys. Rev. **58**, 1098 (1940).
[28] See the Supplemental Material at http://link.aps.org/supplemental/10.1103/PhysRevLett.124.147204 for the justification to neglect the optical phonon and other technical details.
[29] M. Gell-Mann, Phys. Rev. **125**, 1067 (1962).
[30] R. Barnett, G. R. Boyd, and V. Galitski, Phys. Rev. Lett. **109**, 235308 (2012).
[31] K. Ohgushi, S. Murakami, and N. Nagaosa, Phys. Rev. B **62**, R6065 (2000).
[32] Y. He, J. Moore, and C. M. Varma, Phys. Rev. B **85**, 155106 (2012).
[33] G. Go, J.-H. Park, and J. H. Han, Phys. Rev. B **87**, 155112 (2013).
[34] H. T. Ueda, Y. Akagi, and N. Shannon, Phys. Rev. A **93**, 021606(R) (2016).
[35] M. Nakahara, *Geometry, Topology and Physics*, 2nd ed. (Taylor & Francis, London, 2003).
[36] S.-Y. Lee, J.-H. Park, G. Go, and J. H. Han, J. Phys. Soc. Jpn. **84**, 064005 (2015).
[37] R. Matsumoto and S. Murakami, Phys. Rev. Lett. **106**, 197202 (2011).
[38] R. Matsumoto and S. Murakami, Phys. Rev. B **84**, 184406 (2011).
[39] P. A. Joy and S. Vasudevan, Phys. Rev. B **46**, 5425 (1992).
[40] A. Wildes, B. Roessli, B. Lebech, and K. Godfrey, J. Phys. Condens. Matter **10**, 6417 (1998).
[41] M. Banerjee, M. Heiblum, V. Umansky, D. E. Feldman, Y. Oreg, and A. Stern, Nature (London) **559**, 205 (2018).
[42] G. E. W. Bauer, E. Saitoh, and B. J. van Wees, Nat. Mater. **11**, 391 (2012).
[43] R. Cheng, S. Okamoto, and D. Xiao, Phys. Rev. Lett. **117**, 217202 (2016).
[44] S. Murakami and A. Okamoto, J. Phys. Soc. Jpn. **86**, 011010 (2017).
[45] E. Thingstad, A. Kamra, A. Brataas, and A. Sudbø, Phys. Rev. Lett. **122**, 107201 (2019).
[46] S. K. Kim, Y. Tserkovnyak, and O. Tchernyshyov, Phys. Rev. B **90**, 104406 (2014).
[47] I. Dzyaloshinsky, J. Phys. Chem. Solids **4**, 241 (1958).
[48] T. Moriya, Phys. Rev. **120**, 91 (1960).
[49] T. Nomura, X.-X. Zhang, S. Zherlitsyn, J. Wosnitza, Y. Tokura, N. Nagaosa, and S. Seki, Phys. Rev. Lett. **122**, 145901 (2019).
[50] A. B. Sushkov, O. Tchernyshyov, W. Ratcliff II, S. W. Cheong, and H. D. Drew, Phys. Rev. Lett. **94**, 137202 (2005).
[51] C. Manohar and G. Venkataraman, Phys. Rev. B **5**, 1993 (1972).
[52] S. M. Bose, E.-N. Foo, and M. A. Zuniga, Phys. Rev. B **12**, 3855 (1975).
[53] T. Ozawa, H. M. Price, A. Amo, N. Goldman, M. Hafezi, L. Lu, M. C. Rechtsman, D. Schuster, J. Simon, O. Zilberberg, and I. Carusotto, Rev. Mod. Phys. **91**, 015006 (2019).